Journal of Materials Processing Technology 211 (2011) 275–284

Contents lists available at ScienceDirect

Journal of Materials Processing Technology

journal homepage: www.elsevier.com/locate/jmatprotec

Selective laser melting of aluminium components

Eleftherios Louvis*, Peter Fox, Christopher J. Sutcliffe

Department of Engineering, The University of Liverpool, Liverpool L69 3GH, United Kingdom

ARTICLE INFO

Article history:
Received 5 May 2010
Received in revised form
25 September 2010
Accepted 30 September 2010

Keywords:
SLM
Aluminium alloys
Oxidation

ABSTRACT

Previous work has shown that the processing of aluminium alloys by selective laser melting (SLM) is difficult, with reasonable components only being produced with high laser powers (minimum 150 W) and slow laser scanning speeds. The high laser power is a significant problem as it is higher than that used in many SLM machines. Also, the combination of high power and low speed creates a large melt pool that is difficult to control, leading to balling of the melt and possible damage to the powder distribution system. Even when processing is carried out successfully, the high power and slow scan speed significantly increase build time and the manufacturing costs.

This paper considers the changes that can be made to the SLM process so as to reduce the laser power required and increase the laser scanning rates, while still producing components with a high relative density. It also considers why aluminium and its alloys are much more difficult to process than stainless steels and commercially pure titanium. Two MCP Realizer machines were used to process 6061 and AlSi12 alloys, one processing at 50 W and the other 100 W laser power. Even with an optimum combination of process parameters a maximum relative density of only 89.5% was possible (achieved with 100 W). The major confounding factor for processing aluminium and its alloys was found to be oxidation due to the presence of oxygen within the build chamber. This formed thin oxide films on both the solid and molten materials. It was observed that the oxide on the top of the melt pool vaporised under the laser creating a fume of oxide particles, while melt pool stirring, probably due to Marangoni forces, tended to break the oxide at the base of the melt pool allowing fusion to the underlying tracks. However, the oxides at the sides of the melt pool remained intact creating regions of weakness and porosity, as the melt pool failed to wet the surrounding material. Therefore, if 100% dense aluminium components are to be produced by SLM, using low laser powers, methods need to be developed that can either disrupt these oxide films or avoid their formation.

1. Introduction

Selective laser melting (SLM) was originally envisaged as a method of rapid prototyping (RP) enabling the production of complex prototypes directly from metal powders, the components having similar properties to conventionally manufactured ones, rather than just the same physical shape. The industrialisation of this technique has now transformed SLM into a Rapid Manufacturing (RM) process capable of creating bespoke single parts, parts that cannot be made by more conventional routes, and batches of parts where each part in the batch is unique.

SLM creates parts by scanning powdered materials with a laser beam so as to melt and fuse the material into a solid, the parts being manufactured layer by layer direct from the CAD file data. This process has produced some remarkable structures in a fairly wide range of materials, including titanium porous constructs for orthopaedic application (Mullen et al., 2009, 2010), and stainless steel lattice cores for sandwich structures (Shen et al., 2010). However, there have been a number of materials where processing has proved much more difficult, mainly because of the intrinsic metallurgy of the alloy systems.

One materials' group of great interest to those developing the SLM process are the aluminium alloys, which are extensively used in modern manufacturing. These alloys are normally considered to fall into three main categories, heat treatable, non-heat treatable and casting alloys (Polmear, 1995). These main categories can then be broken down by the alloying additions that provide specific properties, mainly due to the formation of different phases and by the use of different heat treatments, if applicable. These heat treatment requirements may affect the suitability of the alloys for SLM, as the melting and refreezing may deleteriously modify the phases present. However, the greatest challenges faced in the SLM processing of aluminium alloys are the same as those faced during conventional manufacturing. Of these the rapid formation of an

* Corresponding author at: Department of Engineering, The University of Liverpool, Harrison Hughes Building, The Quadrangle, Liverpool L69 3GH, United Kingdom. Tel.: +44 0151 794 4911; fax: +44 0151 794 4901.
E-mail addresses: E.Louvis@liverpool.ac.uk, leflouvis@yahoo.gr (E. Louvis).

0924-0136/$ – see front matter © 2010 Elsevier B.V. All rights reserved.
doi:10.1016/j.jmatprotec.2010.09.019

adherent aluminium oxide on any exposed surfaces, whether solid or molten has the most significant effect (Campbell, 2003).

Very little research has been published on the processing of aluminium by SLM. Wong et al. (2007) fabricated heat sinks using 6061 (nominally Al, 0.6 wt% Si, 1 wt% Mg, 0.3 wt% Cu) aluminium powder, but the paper concentrated upon the properties of the heat sinks produced rather than the microstructure and porosity of the parts. Wong et al. state that 6061 was chosen as elemental aluminium had been proved unsuitable by Abe et al. (2001) and because 6061 had been successfully used with SLS and extrusion freeform fabrication. Buchbinder et al. (2008) investigated the SLM processing of AlSi10Mg (nominally Al, 10 wt% Si, 0.35 wt% Mg) parts, producing near 100% dense components and determined a wide range of mechanical properties. This alloy is often used in casting as the near eutectic composition significantly reduces the freezing range (600–555 °C) compared to pure aluminium (660 °C) and 6061 (650–580 °C). The laser beam diameter for their research was 200 μm and it was found that it was possible to produce parts of near 100% relative density only with laser power higher than 150 W. In both these cases, higher laser power and lower scanning speeds were required than when processing metals and alloys with significantly higher melting points. This leads to a disproportional increase in production costs, which considering that aluminium alloys are not expensive, is likely to restrict suitable applications. In addition, such process parameters cannot be implemented with many SLM machines as they have lower laser power capabilities.

There are a number of difficulties in the SLM processing of aluminium powders. Firstly, SLM critically depends on being able to spread a thin powder layer which is difficult because aluminium powders are light with poor flowability, especially in the presence of moisture. This poor flowability often leads to powder bridging inside the hoppers and tubes hindering powder flow. Consequently, aluminium alloy powders are unsuitable for many existing powder deposition mechanisms, even though they are effective for other metal powders of the same particle shape and size distribution.

Secondly, although SLM technology uses shorter wavelength radiation than SLS (1.06 μm compared to 10.6 μm of CO_2 lasers) which favours its absorption by metals (Steen, 2003), the high reflectivity of aluminium (91%) increases the laser power required for melting. This effect becomes more significant with increased beam overlap as although the metal as a powder bed has a high absorptivity (multiple reflections and absorptions within the particle bed modelled by Gusarov and Kruth (2005)), any neighbouring overlapping solidified hatch is highly reflective (Childs and Hauser, 2005) as is the melt bead formed under the laser (Childs et al., 2004). Another reason why higher laser powers are required is the high thermal conductivity of aluminium (compared to other materials used in SLM such as stainless steel and titanium) (Incropera, 2007), which leads to the rapid dissipation of heat away from the scanned location. This phenomenon is most significant during the first layer of the build, which is on the solid aluminium substrate, according to Fischer et al. (2002) who showed that the heat conductivity of powder layers is lower than that of dense materials.

Nevertheless, the main obstacle to the effective sintering and melt processing of aluminium alloys is oxidation. For example, during sintering, the oxide on the surface of particles hinders diffusion (Munir, 1979), while adherent thin oxide films on molten aluminium pacify the surface and reduce wettability. The oxide also causes problems when stirred into the molten metal as this entraps oxide and possibly pores within the material and generates regions of weakness within the component (Campbell, 2003).

Almost all research into the effects of oxide films on aluminium processing has been related to conventional manufacturing processes such as sintering, conventional casting and squeeze casting. However, in comparison, oxidation during SLM may be a much more significant problem, as the powder has a surface oxide film that will be incorporated into the melt pool, the melt pool has an oxide film that affects wetting to surround solid parts, and any previously built solid tracks to the side and below the melt pool will also be covered by oxide films. Not only are these films adherent they can also form at very low oxygen concentrations (10^{-52} pO_2 at 600 °C) (Gaskell, 1995). It is possible therefore that the high laser power needed to process aluminium and its alloys is because of the difficulty in disrupting these oxide films rather than a problem in melting the metal.

In this paper the authors attempt to clarify the importance of oxide films in the SLM processing of aluminium and its alloys, and identify methods for increasing part density without the use of excessive laser powers. Therefore, the work is aimed at producing increasingly dense parts while using high scanning speeds and laser powers lower than 150 W, which has been shown to be the minimum necessary to eliminate porosity from the parts.

2. Materials and methods

Two MCP Realizer 100 (MTT Tooling Technologies, UK) SLM machines were used for this work, one with a maximum laser output of 50 W and the other 100 W. The operating principle of the MCP Realizer machines is shown in Fig. 1. These machines used a non-standard powder deposition mechanism to allow them to handle powders with poor flowability like aluminium. A hopper metering mechanism was used to deposit powder piles in front of a wiper blade that spread the powder on the built area to form a thin uniform layer. An optical system was used to direct (positional accuracy 5 μm) the ytterbium fibre laser beam (λ = 1.06 μm) with nominal diameter of 80 μm onto the built area, where it was focused. The parts were built layer by layer on an aluminium substrate with the help of an elevator that moved the substrate downwards by a distance equal to the layer thickness. The process was carried out under an argon atmosphere with an overpressure of 10–12 mbar and oxygen level of 0.1–0.2%. A filtering mechanism was used to clean particulates from the atmosphere, which was circulated by a pump.

Prior to the production of an SLM part, a number of basic geometrical features such as the point sequence, the border geometry, the hatch geometry, and the support geometry, need to be specified. The correct optimisation of all these features is carried out by taking into consideration various properties such as the part's surface finish and microstructure, its mechanical properties, and

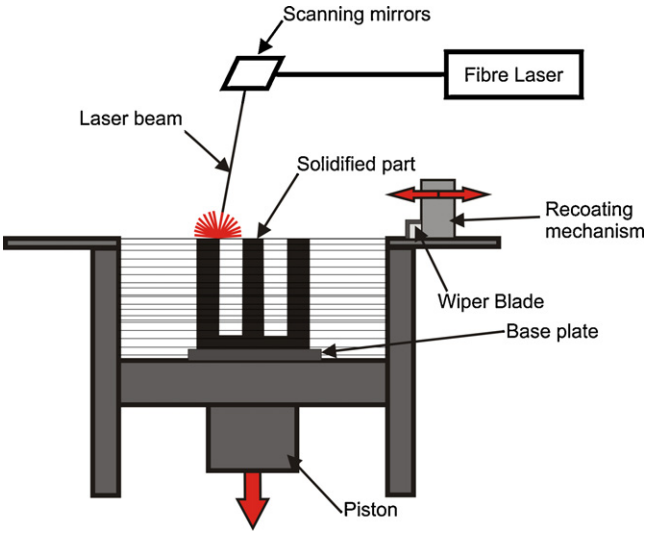

Fig. 1. SLM operating principle.

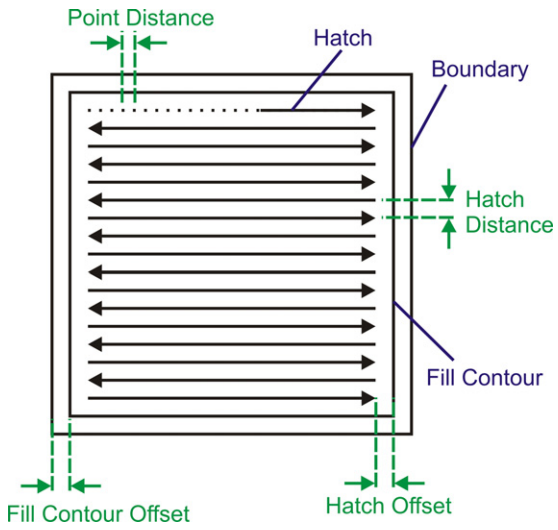

Fig. 2. Basic laser scanning parameters.

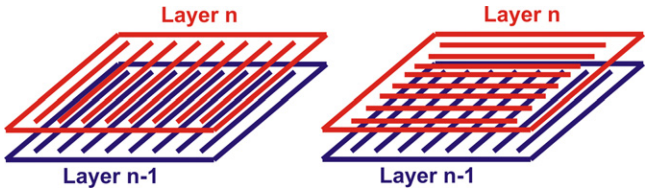

Fig. 3. Scan orientation altered by 90 °C at each layer.

the production time and cost. However, the most important target when introducing a new material to the process is the production of fully dense parts.

The basic process parameters that can be controlled are the laser power, the point distance between the focused laser spots during scanning, the exposure time that it resides at each point (in other words the laser scan speed: point distance/exposure), and the distance between the laser hatches (Fig. 2). However, the MCP Realizer machines allow the modification of several other parameters, such as the use of different scanning patterns, the scan orientation at each layer (Fig. 3), and the boundary scanning parameters (Fig. 2).

The laser power selected in each case was the highest output of the two SLM machines (50 and 100 W). Cubic specimens 10 mm × 10 mm × 10 mm (Fig. 4) were built using combinations of

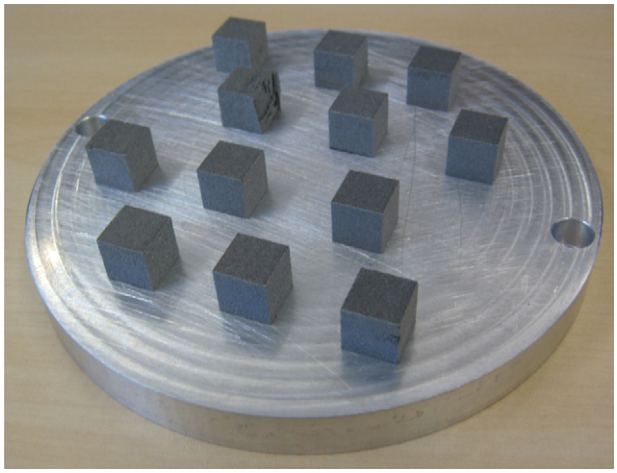

Fig. 4. SLM 10^3 mm^3 cubic aluminium specimens on aluminium SLM build substrate.

the other parameters, and their relative density was determined gravimetrically. The scanning direction was kept the same for every layer in order to make the scan tracks easier to observe and the built plate (substrate) was heated to 180 °C. The layer thickness was set to a typical value of 50 μm as recommended for 45 μm average particle diameter powders.

Optical micrographs were obtained using a Nikon Epiphot optical microscope after polishing the samples down to 50 nm using standard metallographic techniques (Metaserv Universal Polisher) and etching them subsequently with Keller's reagent (aqueous solution of 1 vol% hydrogen fluoride, 1.5 vol% hydrochloric acid and 2.5 vol% nitric acid). For higher magnifications an SEM (Hitachi S-246N, Japan, resolution 10 nm) was used. To examine material ejected from the powder bed during processing, 3 mm diameter copper TEM grids with carbon films were used to collect particulates. Analysis of these materials was carried out using a JEOL 2100FCs Transmission Electron Microscope for collecting images of the different features found on the grids. EDS analysis was carried out using an EDAX Genesis 4000 system for these TEM samples to determine the composition of the regions.

The aluminium alloy that was used during most experiments was 6061, although for some experiments AlSi12 was selected. This is a near eutectic casting alloy and was used to determine the influence of melting point and the castability of the alloy upon SLM processability.

3. Results

The relationship between the part density, whose increase is the primary aim of the current research, and the input parameters for the process was examined. Furthermore, the effect of oxidation on the resulting part density was investigated; this included analysis of the way that the oxide formed during laser scanning.

3.1. Process parameters development for aluminium alloys

Initially, research was carried out using a MCP Realizer 100 machine operating at 50 W laser power, processing a 6061 aluminium alloy powder. After initial configuration of the system, the process parameters were altered in a systematic way to identify the settings that resulted in insufficient melting, or delamination of the layers, so as to define a process map. The scanning speeds were set by combining the point distances 65, 75 and 85 μm and varying exposure times of intervals (200 μs). Then, they were applied to various hatch distances resulting in different relative densities of the part (Fig. 5). It was observed that for this aluminium alloy, balling of the melt pool was a significant problem, especially at low scanning speeds. The surface profilimetry scans (OSP 100 surface profiler) on Fig. 6 show that low scan speeds generate roughness greater than the set layer thickness. On the other hand, high scanning speeds led to lower relative densities due to insufficient powder melting. Consequently, for the majority of the hatch distances, the higher values of the relative density were observed within a narrow speed range (100–200 mm/s), the highest being 83.7% at 0.15 mm hatch distance.

This is similar to the work of Olakanmi et al. (2009) who scanned single layers of Al, Al–Mg and Al–Si powders with a CO_2 laser (600 μm beam diameter) using combinations of laser powers and scanning speeds. Their investigation of the resulting surface morphologies revealed a narrow process parameter window where minimum balling occurred, with high energy densities creating large agglomerates. It was suggested that the cause of this balling phenomenon was the excessive size of the melt pool accompanied by a long liquid lifetime. Decreasing the energy density by increasing the laser scanning speed proved to be beneficial for the

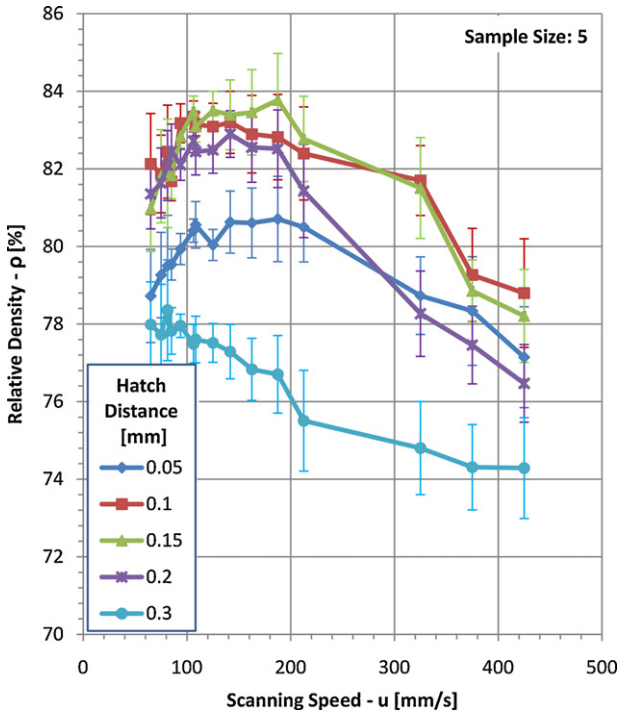

Fig. 5. Effect of the main SLM parameters (laser scanning speed, hatch distance) on the resulting relative density of 6061 at 50 W.

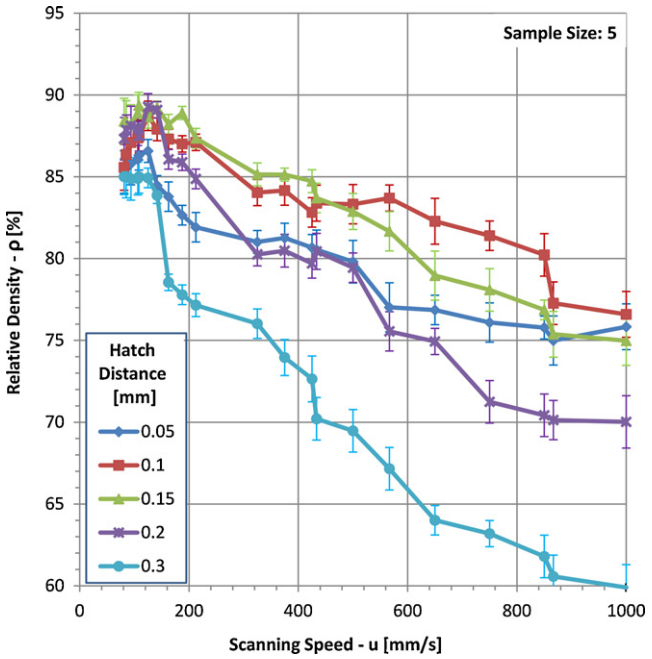

Fig. 7. Effect of the main SLM parameters (laser scanning speed, hatch distance) on the resulting relative density of 6061 at 100 W.

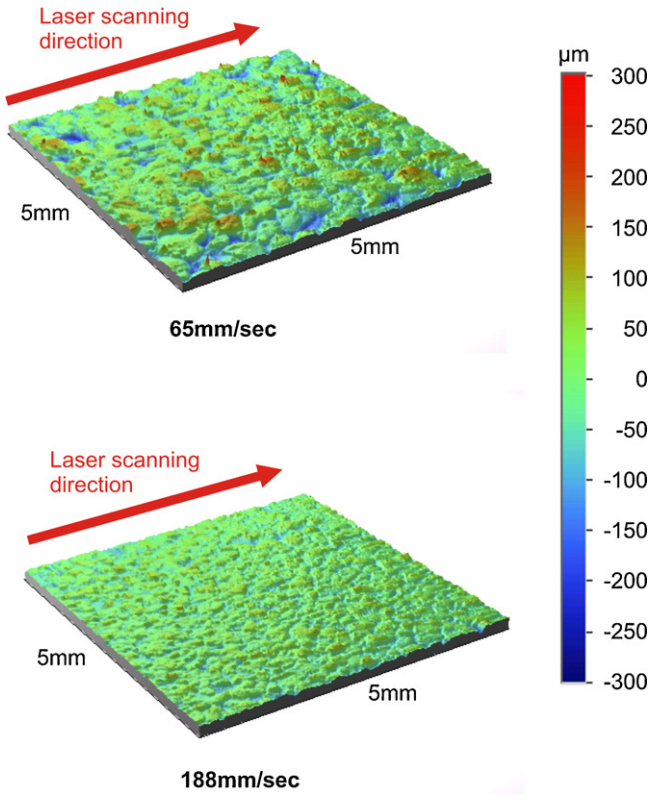

Fig. 6. Top surface roughness profile of 6061 samples that were made using different laser scanning speeds. The rest of the SLM process parameters that were used were the same; laser power 50 W, hatch distance 0.15 mm.

smoothness of the generated laser hatch lines. However, further increase of the laser scanning speed led to the breakage of the molten track into a series of balls due to Rayleigh instability.

The experiments were repeated with a laser power of 100 W (Fig. 7) and it was observed that the increase in power increased the maximum relative density by 5%. This result suggests that aluminium alloys require significantly higher laser powers than needed to process powdered metals with significantly higher melting points, the MCP Realizer being able to process steel with a laser power of 50 W.

At both power settings, 50 and 100 W, hatch distances greater than 0.3 mm resulted in delamination (Fig. 8). Balling was also present in the case of 100 W at low scanning speeds as shown by the surface profilimetry scans in Fig. 9. Again, here the highest relative densities are located within a narrow range of scanning speeds

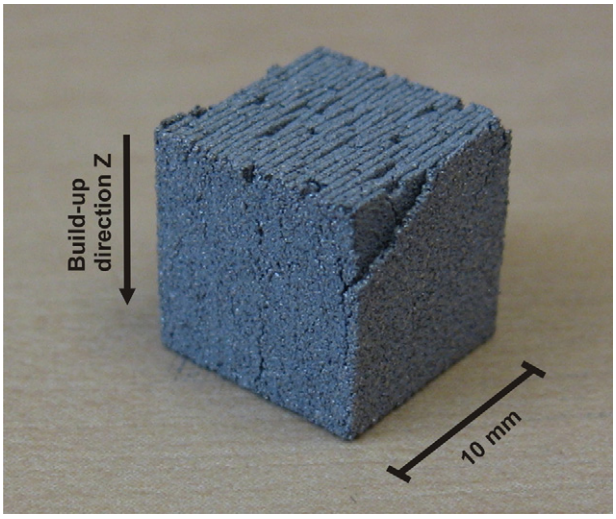

Fig. 8. Wall delamination shown at the bottom surface of a 6061 specimen made at 50 W laser power; the selected hatch distance is 0.4 mm, which is larger than the limit imposed by the molten track width.

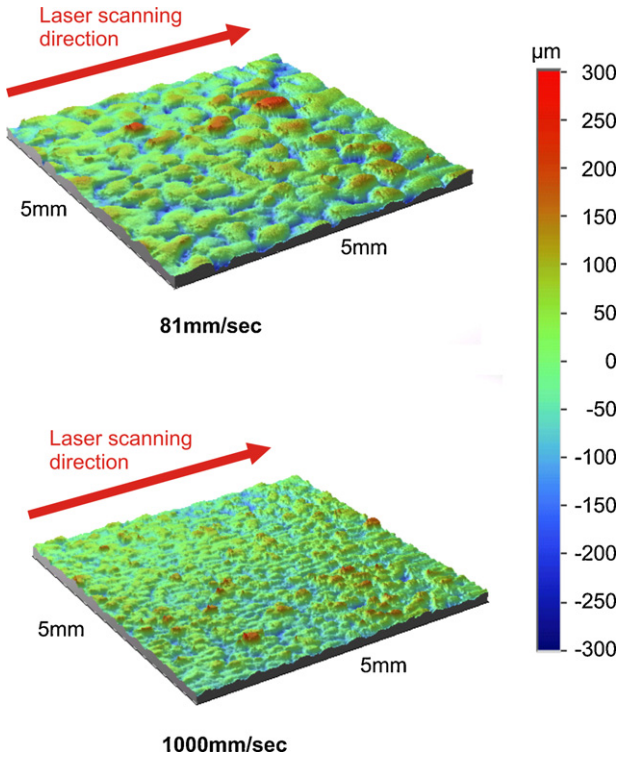

Fig. 9. Top surface roughness profile of 6061 samples that were made using different laser scanning speeds (laser power 100 W, hatch distance 0.15 mm).

100–200 mm/s. At higher speeds than these, the overlapping area of two adjacent melt tracks reduces resulting in increased porosity, especially at large hatch distances. On the other hand, increasing the overlapping area was also limited, as the density was reduced at hatch distances below 0.1 mm.

AlSi12 was also investigated using the same laser powers and was found to produce similar results even though its melting point is significantly lower (Fig. 10). As the curves have a similar shape to those obtained with 6061, only the speed range of the previously found higher density values was examined, and the hatch distances greater than 0.3 mm and less than 0.05 mm were also excluded. However, although increasing laser power from 50 to 100 W resulted in an increase in the relative density as with the

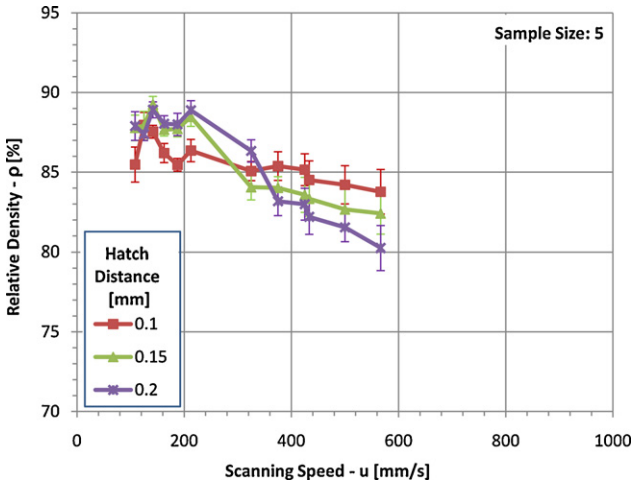

Fig. 10. Effect of the main SLM parameters (laser scanning speed, hatch distance) on the resulting relative density of AlSi12 at 100 W.

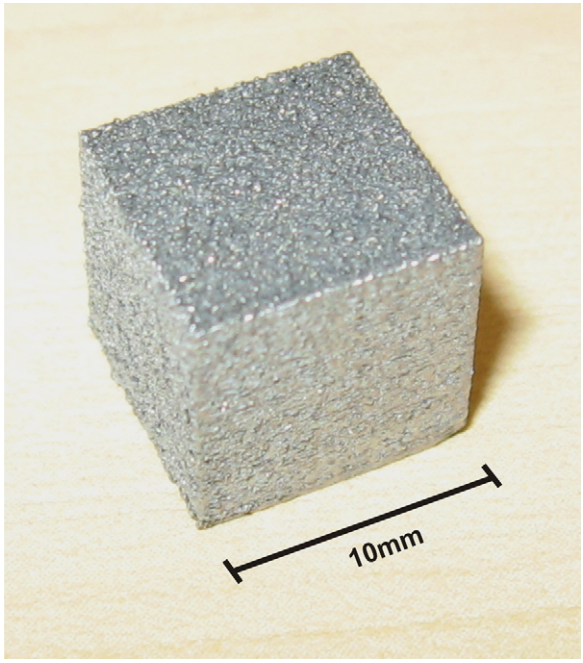

Fig. 11. Top surface discolouration of an SLM 6061 sample.

6061 alloy, neither material reached a relative density higher than 89.5%.

As stated earlier, the difficulty in processing aluminium may be due to its high reflectivity reducing its heating, or its high thermal conductivity allowing rapid loss of heat. However, overcoming these problems by increasing the incident laser power still leaves those caused by the formation of oxides, and if these cannot be either vaporised or stirred into the melt pool, the melt pool will fail to fuse and wet to the surrounding solid, creating a porous structure. As it seemed unlikely that this system cannot fully melt an AlSi12 alloy with a 100 W laser, the role of oxidation in modifying the behaviour of aluminium alloys during SLM processing was investigated further.

3.2. Oxidation during SLM of aluminium

During processing, the overall gas oxygen level of the MCP Realizer 100 as well as many other SLM machines is 0.1–0.2%. This is low enough to allow the processing of stainless steel and titanium, probably because the oxides formed are either easier to break up and so enter the melt pool or because they are vaporised during heating by the laser. However, the effect of the oxygen still present in the chamber on the aluminium specimens can be seen on their top surfaces which are discoloured compared to the other surfaces (Fig. 11). As this discolouration is always seen on the top of the specimen it must also occur on each of the scanned layers during the process.

Examination of fracture surfaces created by breaking the 6061 samples (Fig. 12A) showed regions that were flat or faceted and very dissimilar to regions where plastic deformation had occurred. These flat regions are, when examining the fracture surfaces of castings, considered to be indicative of the presence of thin oxide films. Also observed on the fracture surface was powder which had not been incorporated into the melt, and as this had a similar morphology to the original powder used, it is likely that it was trapped in pores or voids in the sample when depositing the next layer (Fig. 12B).

To determine the level of oxide present within the samples they were deep etched using a solution of sodium hydroxide (40 wt%

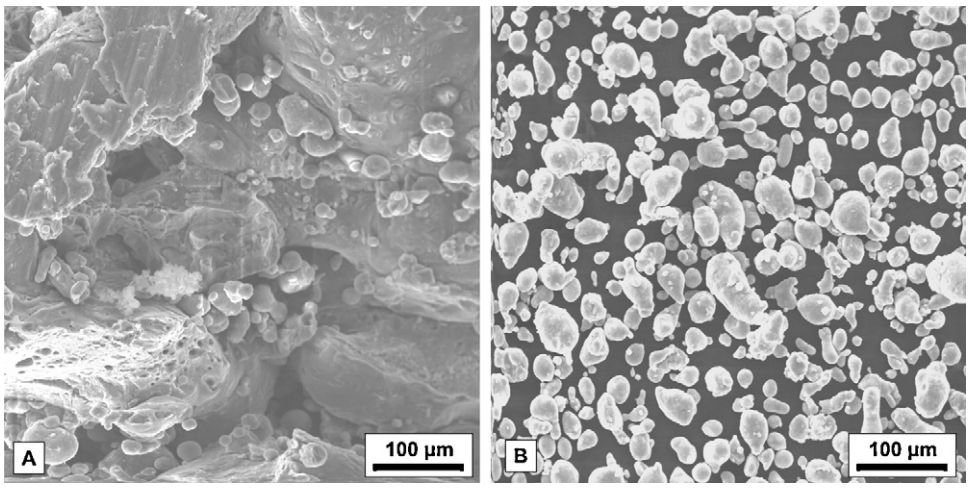

Fig. 12. SEM micrographs of aluminium alloy 6061; (A) fracture surface of an SLM sample; (B) sample of 6061 powder.

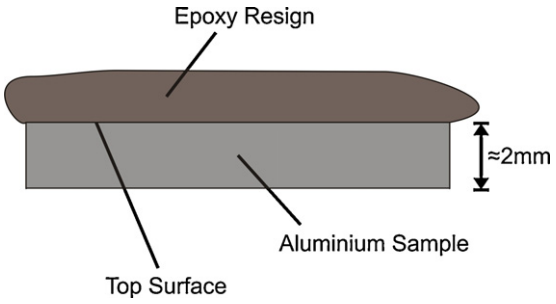

Fig. 13. SLM specimen used for revealing the oxide by inserting it into NaOH solution.

NaOH). This solution reacts strongly with aluminium taking it into solution but does not react with aluminium oxide, allowing any oxide to be retrieved. To retrieve the oxide layer on the top of the specimens blocks (as seen in Fig. 11) thin 6061 SLM specimens (Fig. 13) had an epoxy resin bonded to the top surface and then the alloy dissolved. However, instead of observing the thin layer from the very top of the specimen it was seen that oxide layers were present between the laser hatches (Fig. 14). It appears therefore that although bonding was occurring between the layers with the oxides breaking up this was not true between tracks.

3.3. Compositional analysis of produced fumes

To investigate the role of oxygen in the processing of aluminium alloys further it was decided to examine the materials within the 'fumes' that are formed when the laser melts the powder bed. The particles within the fumes were collected on thin carbon films mounted on copper grids. The alloy used for these experiments was 6061 and a laser power of 50 W. The grids where placed close to the outlet of the process chamber where the fumes are directed by the gas circulation system. Fairly small particles (5–10 μm) on the grid were easily identified using TEM techniques (Fig. 15), and their chemical composition was identified by EDS analysis, which showed them to be predominantly aluminium with no detectable oxygen (Fig. 16). Given that the oxygen level of the SLM process chamber (0.1–0.2%) is sufficient for some oxidation to occur and that these particles are similar in size and shape to the original 6061 powder (Malven Mastersizer 2000, UK), it is likely that they are from the powder bed not the fume. Similar work carried out by Gill (2006) analysed particles formed in the fume generated by femtosecond laser ablation of aluminium. They detected spherical particles (10–800 nm diameter) with little or no oxidation when processing under helium and highly oxidised non-spherical debris when processing under air.

The copper grids also contained much smaller clusters of particles, in a similar size range (10–20 nm) to those observed by Gill, that were more likely to have formed in the fume (Fig. 17).

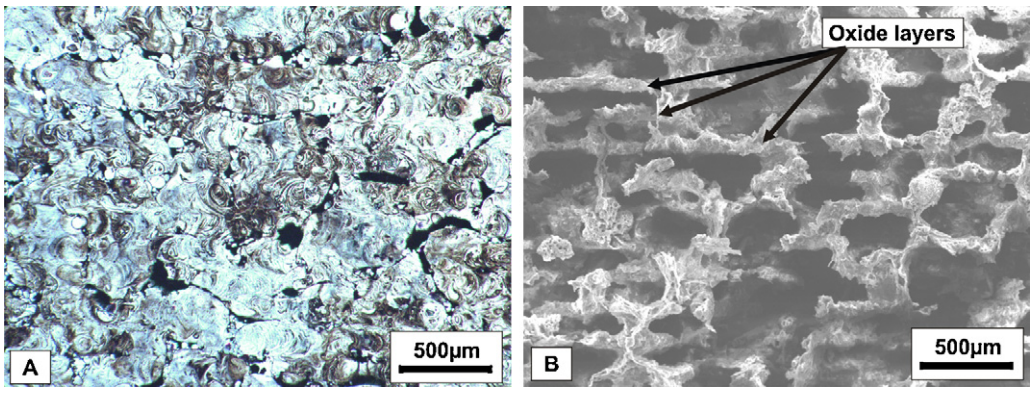

Fig. 14. Optical and SEM Micrographs of a 6061 sample section; (A) sample after polishing and etching with Keller's reagent; (B) deep etched with NaOH solution.

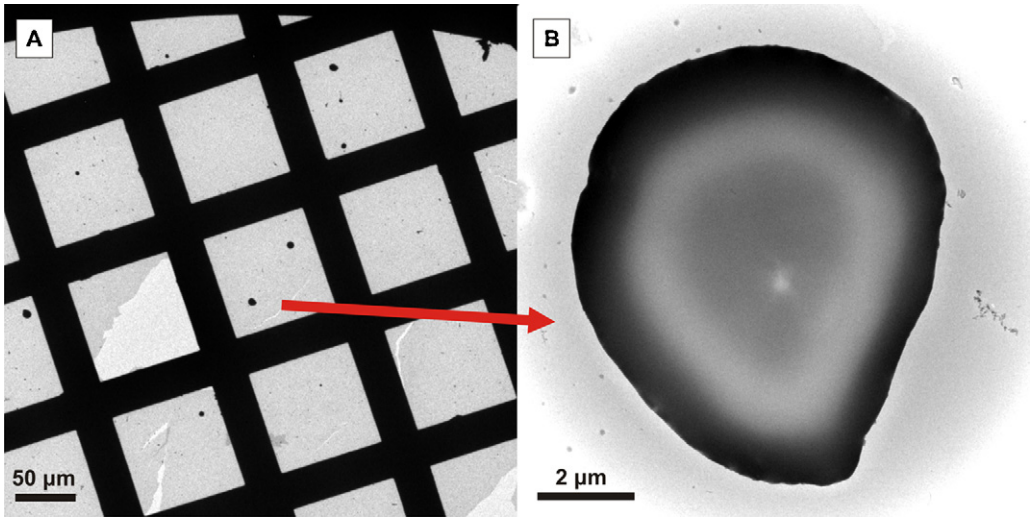

Fig. 15. TEM micrographs of aluminium particles found on the copper grids; (A) large dense particles, clearly observed at low magnifications (50×), such as the two in the centre grid location of this micrograph; (B) lower left particle of the centre grid location of (A).

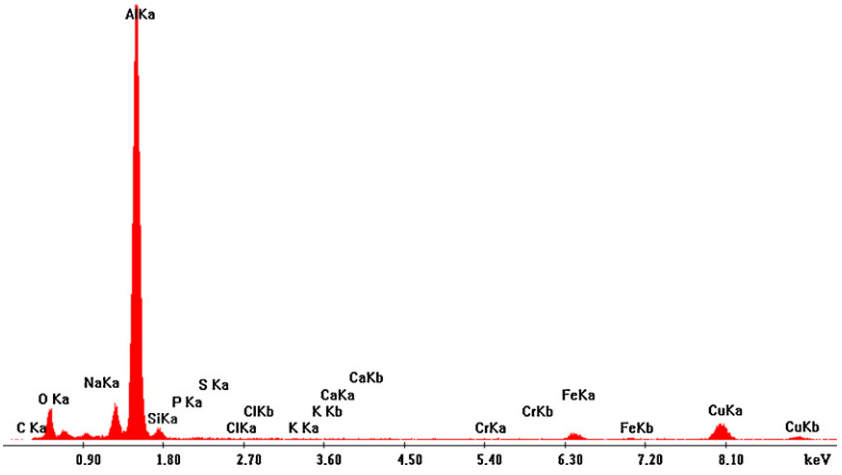

Fig. 16. EDS Spectrum of the aluminium particles found on the copper grids.

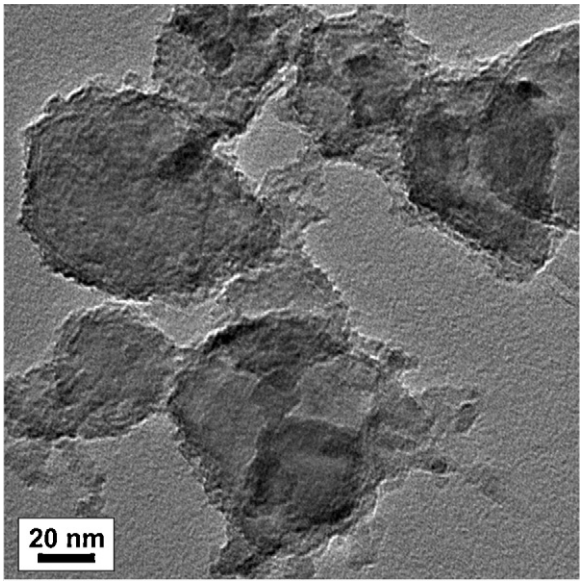

Fig. 17. TEM micrograph of the fumes collected on the sample grids.

These particles often contained aluminium, magnesium and oxygen (Fig. 18A) with a magnesium content significantly higher than that of the alloy (copper was also observed in the spectra but this was from the copper TEM grids). Analysis of other particles showed clusters that were predominantly Mg and O, and were likely to be magnesium oxide (Fig. 18B). The fume therefore is either metal that is vaporised from the surface and subsequently oxidised within the chamber, oxide that has vaporised from the powder particles upon heating by the laser but before the molten metal enters the melt pool, or oxide vaporised from the surface of the melt pool. Given the low magnesium content of this alloy (6061) and the high magnesium content of the particles in the fume it is more likely that these are formed by the evaporation of surface oxides which are likely to be mixed aluminium magnesium oxides.

4. Discussion

It can be seen from this work that during the SLM processing of aluminium and its alloys significant amounts of oxide are incorporated into the parts. It follows therefore that the quality of aluminium or aluminium alloy parts produced by SLM is controlled by the formation of oxide films in a similar way to conventional

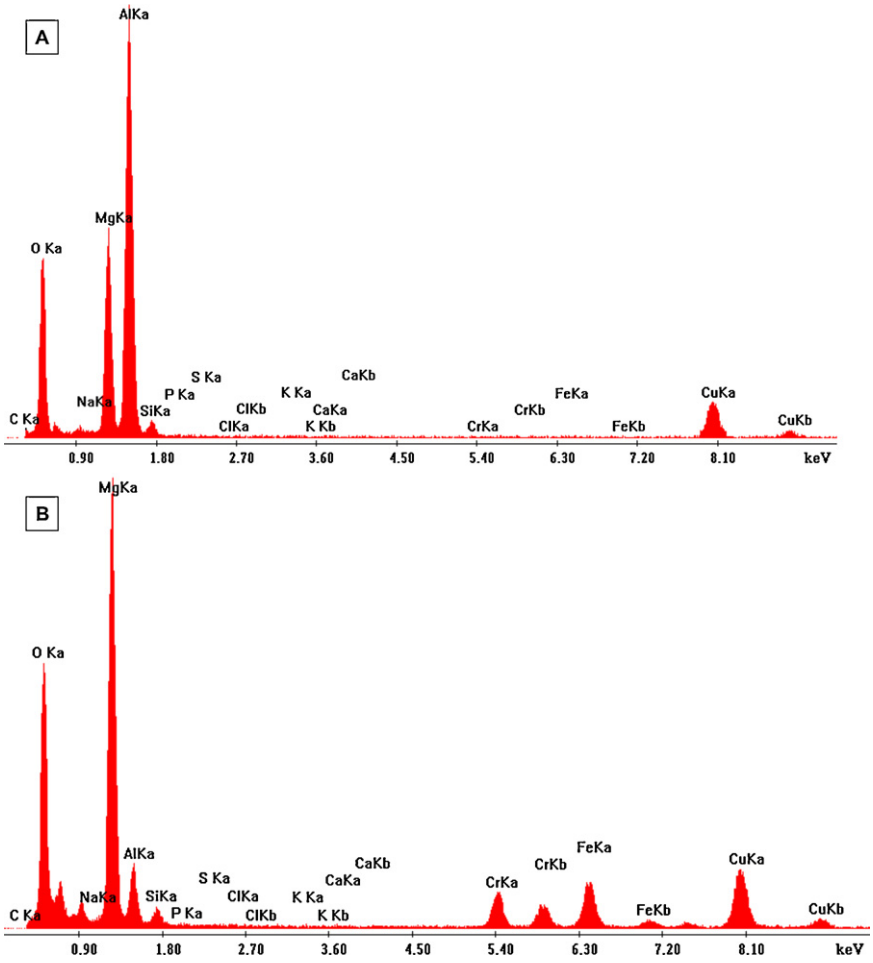

Fig. 18. EDS Spectra of the fumes.

casting and that an understanding of the behaviour of these films and how to disrupt them is pivotal to improving the parts. Disruption rather than avoidance seems the most likely course of action purely because they are difficult to avoid, the dissociation pressure of alumina being 10^{-52} pO_2 at the melting point of aluminium. Although the constant reaction between the alloy and the atmosphere as the material is processed will reduce the oxygen content of the gas by forming oxides, even at very low oxygen concentrations oxide films will form. These oxide films have a number of effects including passivating the surface of the molten metal, reducing its reactivity and increasing the difficulty of penetrating the surface, while actually lowering the surface tension (Sarou-Kanian et al., 2003).

The creation of a part by SLM can be considered as the movement of a melt pool across a surface by the addition of powder at the front of the pool and the freezing of material at the back. If the component produced is to be 100% dense it is important that the underlying and surrounding solid partially remelts so that the regions wet and fuse with the melt pool. However, with aluminium and its alloys this description is incomplete as there is an adherent solid oxide layer formed both on the underlying solid and on the melt pool, and even when sufficient heat is applied to partially remelt the underlying metal there are still two thin oxide films separating the regions of molten metal. Therefore the wetting and fusing of the aluminium regions is controlled by the disruption or disassociation of these oxides, not by the melting of the different regions.

The effect of these oxides can be seen in Fig. 14B. In this case they appear as walls parallel to the scan direction and as the scans in each layer lie over each other, the walls extend up the specimen. If the samples were produced with the more conventional cross hatching, where alternate layers would be scanned at 90 degrees to each other, the oxides would be less obvious as they would tend to break up during the deep etching. They would, however, still be present within the material and may act as lines of weakness.

The oxide films in the deep etched specimens appear rather wide, especially as they are not visible in the conventional metallographic cross section (Fig. 14A). This is because each wall consists of two thin oxide films separated by a gap in which there will be unmelted powder and trapped regions that form pores. In the conventionally prepared metallographic samples the oxide films cannot be observed but it can be seen that the porosity is mainly present in these regions. The presence of the walls tends to suggest that the oxides films break up on the top and bottom surfaces of the melt pool but not to the sides.

It is likely that the temperature of the upper molten surface under the laser beam is high enough to vaporise the oxide film on the top of the melt pool, and it is this that leads to the high level of magnesium in the fume particles analysed. However, the oxides films that control wetting are those below and to the sides of the melt pool not those on the top, as it is here that the regions fuse to form the solid. The fusing of these regions requires the wetting of one oxide coated molten metal region with another and therefore is similar to wetting experiments carried out between molten aluminium and alumina.

Laurent et al. (1988) considered the wetting of aluminium to alumina and showed that under high vacuum conditions the contact

angle between the liquid aluminium and the alumina decreased linearly with increased temperature until a particular fairly poorly defined temperature when wetting would increase rapidly. This behaviour was thought to occur because the molten metal is surrounded by a thin oxide film that controls the wetting process and as such the process at reasonably low temperatures is slow, at 973 K (vacuum of 5×10^{-5} Pa) it took 1000 s for the wetting angle to reach 108°. At higher temperatures rapid wetting was observed and it was proposed that the oxide vaporised by the formation of Al_2O. The very high temperatures and long holding times required for wetting have been confirmed by others (Rocha-Rangel et al., 2003). Levi and Kaplan (2002) also concluded that there is a reduction of the contact angle of Al on α-Al_2O_3 at higher temperatures, which depends on the oxygen partial pressure.

Although the dissociation of the film and the formation of Al_2O may play a part in conventional sintering it is unlikely to be important in SLM as the time when the metal is molten is much shorter than the time required for the mechanism to work. It is also difficult to see why the oxide film would dissociate on the lower surface but not the sides. Therefore it is likely that another mechanism is at work probably one that disrupts the oxides by stirring the molten metal, so as to fold the oxide into the melt and expose unoxidised molten metal that can bond to its surroundings. The most likely force that could drive this stirring is the Marangoni force.

The flow of molten metal under the influence of Marangoni forces is caused by local differences in surface tension of the liquid's surface, and this in turn is affected by the difference in temperature in different regions of the melt pool. The melt pool is maintained under the laser by the addition of powder and the freezing of solid and as such there is a significant temperature gradient along the melt pool but there is likely to be less difference in temperature across it. How the Marangoni forces affect the flow of metal and therefore the shape of the melt pool is a function of whether the surface tension increases or decreases with temperature and for most materials this is significantly affected by impurities, as is seen when steel is welded in atmospheres with different oxygen or carbon dioxide impurity levels (Lu et al., 2004). With aluminium the vaporisation of the oxide film on the top of the melt pool will increase the surface tension here relative to the sides, and this combined with the effects of the temperature profile will produce stirring within the melt pool that probably breaks up the oxide films on the base but not the sides. It is often seen in welds that if the change in surface tension with temperature is greater than zero a deep narrow weld is produced as liquid is drawn from the sides of the weld to the middle (Lu et al., 2008). This appears to be similar to the process observed here, where the oxides formed at the side of the melt pool are unaffected but those below seem to be broken (Fig. 19). The success in processing aluminium and its alloys with very high laser powers may be due to changes in the melt pool size and changes in the liquid flows within the melt pool at the higher temperatures induced.

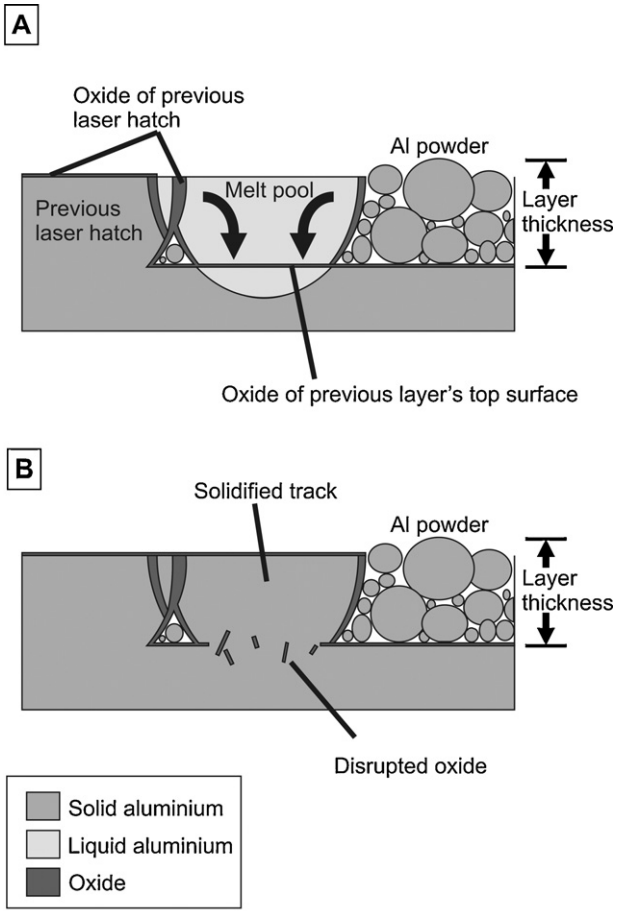

Fig. 19. (A) Marangoni convection in the melt pool. (B) Oxide disruption and solidification of the melt pool.

5. Conclusions

The difficulties encountered when SLM processing aluminium and its alloys appear to be caused by thin oxide films, and in many ways these defects are the same as those seen in conventional casting. The formation of oxide films on both solid and liquid metal surfaces leaves oxides films between the laser hatches at every layer of the aluminium parts and where two oxide films meet then pores are formed. As it is unlikely that the formation of oxide films can be avoided completely the SLM process must break up these oxides if 100% dense parts are to be formed, and this is what allows high density parts to be built with high laser powers. The oxide film on the upper surface of the melt pool evaporates under the laser beam but on the other surfaces it remains intact. Marangoni forces that stir the melt pool are the most likely mechanism by which these other oxide films are disrupted and with these experiments the melt pool seems to disrupt the lower oxide films but not the sides, creating the 'walls' of oxides.

Therefore further research on the SLM of aluminium should be primarily orientated towards new methods of controlling the oxidation process and disrupting oxide films formed within the components.

Acknowledgements

The authors would like to thank the Engineering and Physical Science Research Council (EPSRC) for their financial support (grant number EP/C009398/1). Continuous support was also provided by MTT Technologies.

References

Abe, F., Osakada, K., Shiomi, M., Uematsu, K., Matsumoto, M., 2001. The manufacturing of hard tools from metallic powders by selective laser melting. Journal of Materials Processing Technology 111 (1–3), 210–213.

Buchbinder, D., Meiners, W., Wissenbach, K., Müller-Lohmeier, K., Brandl, E., 2008. Rapid manufacturing of aluminium parts for serial production via selective laser melting (SLM). In: Hirsch, J. (Ed.), Proceedings of the 11th International Conference on Aluminium Alloys. Aachen, Germany, pp. 2394–2400.

Campbell, J., 2003. Castings, 2nd ed. Butterworth-Heinemann, Oxford.

Childs, T.H.C., Hauser, C., 2005. Raster scan selective laser melting of the surface layer of a tool steel powder bed. Proceedings of the Institution of Mechanical Engineers, Part B: Journal of Engineering Manufacture, 379.

Childs, T.H.C., Hauser, C., Badrossamay, M., 2004. Mapping and modelling single scan track formation in direct metal selective laser melting. CIRP Annals – Manufacturing Technology 53 (1), 191–194.

Fischer, P., Karapatis, N., Romano, V., Glardon, R., Weber, H.P., 2002. A model for the interaction of near-infrared laser pulses with metal powders in selective laser sintering. Applied Physics A: Materials Science and Processing 74 (4), 467–474.
Gaskell, D.R., 1995. Introduction to the Thermodynamics of Materials, 3rd ed. Taylor & Francis, Washington.
Gill, M.D.H., 2006. Micro and nano structuring of metals using femtosecond laser ablation. Ph.D. Thesis, University of Liverpool.
Gusarov, A.V., Kruth, J.P., 2005. Modelling of radiation transfer in metallic powders at laser treatment. International Journal of Heat and Mass Transfer 48 (16), 3423–3434.
Incropera, F.P., 2007. Introduction to Heat Transfer, 5th ed. John Wiley & Sons, New York.
Laurent, V., Chatain, D., Chatillon, C., Eustathopoulos, N., 1988. Wettability of monocrystalline alumina by aluminium between its melting point and 1273 K. Acta Metallurgica 36 (7), 1797–1803.
Levi, G., Kaplan, W.D., 2002. Oxygen induced interfacial phenomena during wetting of alumina by liquid aluminium. Acta Materialia 50 (1), 75–88.
Lu, S., Fujii, H., Nogi, K., 2008. Marangoni convection and weld shape variations in He–CO_2 shielded gas tungsten arc welding on SUS304 stainless steel. Journal of Materials Science 43 (13), 4583–4591.
Lu, S., Fujii, H., Nogi, K., 2004. Marangoni convection and weld shape variations in Ar–O_2 and Ar–CO_2 shielded GTA welding. Materials Science and Engineering A 380 (1–2), 290–297.
Mullen, L., Stamp, R.C., Brooks, W.K., Jones, E., Sutcliffe, C.J., 2009. Selective laser melting: a regular unit cell approach for the manufacture of porous, titanium, bone in-growth constructs, suitable for orthopedic applications. Journal of Biomedical Materials Research – Part B: Applied Biomaterials 89 (2), 325–334.
Mullen, L, Stamp, R.C., Fox, P., Jones, E., Ngo, C., Sutcliffe, C.J., 2010. Selective laser melting: a unit cell approach for the manufacture of porous, titanium, bone in-growth constructs, suitable for orthopedic applications. II. Randomized structures. Journal of Biomedical Materials Research – Part B: Applied Biomaterials 92 (1), 178–188.
Munir, Z.A., 1979. Analytical treatment of the role of surface oxide layers in the sintering of metals. Journal of Materials Science 14 (11), 2733–2740.
Olakanmi, E.O., Cochrane, R.F., Dalgarno, K.W., 2009. Spheroidisation and oxide disruption phenomena in direct selective laser melting (SLM) of pre-alloyed Al–Mg and Al–Si powders. In: TMS 2009 – 138th Annual Meeting and Exhibition, February 15–19, 2009, San Francisco, CA, USA, p. 371.
Polmear, I.J., 1995. Light Alloys: Metallurgy of the Light Metals, 3rd ed. Arnold, London.
Rocha-Rangel, E., Becher, P.F., Lara-Curzio, E., 2003. Reactive-wetting of alumina by molten aluminum alloys. In: Advanced Structural Materials Symposium of the Annual Congress of the Mexican Academy of Materials Science, August 26–31, 2002, Cancun Quintana Roo, Mexico, p. 97.
Sarou-Kanian, V., Millot, F., Rifflet, J.C., 2003. Surface tension and density of oxygen-free liquid aluminum at high temperature. International Journal of Thermophysics 24 (1), 277–286.
Shen, Y., McKown, S., Tsopanos, S., Sutcliffe, C.J., Mines, R.A.W., Cantwell, W.J., 2010. The mechanical properties of sandwich structures based on metal lattice architectures. Journal of Sandwich Structures and Materials 12 (2), 159–180.
Steen, W.M., 2003. Laser Material Processing, 3rd ed. Springer, London.
Wong, M., Tsopanos, S., Sutcliffe, C.J., Owen, I., 2007. Selective laser melting of heat transfer devices. Rapid Prototyping Journal 13 (5), 291–297.